MRI Morphological and Diffusion Tensor Imaging (DTI) Analysis to Early Alzheimer Disease

Y. Zhou[1], Y. Ge[1], and J. H. Dougherty[2]

[1]Radiology/Center for Biomedical Imaging, New York University School of Medicine, New York, NY, United States, [2]Medicine and Cole Neuroscience Center, University of Tennessee Medical Center at Knoxville, Knoxville, TN, United States

Introduction: Shape and thickness measures can provide us local morphological information; together with microstructural information from diffusion tensor imaging (DTI), this study was to determine whether there are morphological and intrinsic microstructural changes of medial temporal lobe and striatal structures in patients with early Alzheimer's disease (AD) using shape and thickness analysis.

Methods: Nine early AD patients (MMSE 19 – 24) and nine age-matched normal controls were included. High-resolution three-dimensional T1-MPRAGE (176-slice with 1mm isotropic spatial resolution) and DTI images (12 directions and 3 b-values: b=0, 500 s/mm^2, 1000 s/mm^2) were acquired on 1.5T. Medial temporal lobe (MTL) structure and striatum mask images underwent shape and thickness analysis based on MPRAGE images using algorithms and software from [1]. The following 17 structures were manually drawn and studied: four ROIs within MTL including amygdala (AMY), entorhinal (ENT), hippocampus (HPC) and parahippocampus (PIP); three striatum ROIs including dorsal caudate (DCA), dorsal putamen (DPU) and ventral striatum (VST); thalamus (THL) on both sides and left posterior cingulate (PCC). For DTI data, fractional anisotropy (FA) images were computed and averaged over each ROI for group comparison.

For shape analysis, the binary ROI mask images of each structure generated from MEDx (for delineation on MPRAGE images) were converted to the NIFTI_GZ format, transformed to the standard MNI-2mm template space and then processed through the standard pipeline procedure in the following way: First, Gaussian smoothing was applied to each binary ROI, followed by the spherical surface mesh and parameterization and also the subdivision approximation based on partial differential equations for surface projection representation. Next, each ROI's meshing parameter was scaled with each subject's intracranial volume (a factor of 1.1 to 1.6) and a nonparametric statistical test using default values (20000 for permutation number, 1000 for significance steps, and 0.5 for correction step) was performed to achieve 0.5% significance correction resolution for group comparison.

For thickness analysis, the brain volume images of each subject were first generated after extracranial contents stripping using FSL-BET followed by gray and white matter segmentation using the FSL "fast" tool on images with an isotropic resolution of 1mm. Then the gray and white matter mask images went through the standard cortical thickness mesh step from the shape analysis tool to generate the boundary and inside cortical thickness map, the gray matter Danielson map and white matter distance map metrics. For across-subject quantification, the four metric images were scaled to each subject's intracranial volume (a factor of 1.1 to 1.6) and then multiplied by a 1.5 factor to achieve an approximate 1 scale. The average thickness or distance measure of each ROI was done by the average of the scaled metric images within these ROIs for each subject.

Results: Figure 1 showed the statistical results of comparison significance maps between AD and age-matched normal control populations based on shape analysis for the eight ROIs on the left side of the brain (right side not shown). Distributed medial deformations were seen at the AMY, DPU and THA, with slight medial deformations at DCA, PCC and PIP and slight tail deformations at the ENT and HPC regions.

For gray matter thickness measurements, overall, the declines in gray matter thickness were seen in the dorsal medial temporal lobe and the anterior striatum regions in early AD. And most thickness change comes from the AMY, DCA, ENT, THA and VST, with no statistical differences found from the HPC, PIP and DPU regions. A strong negative correlation exists (r = -0.91, p < 0.001) between the inside cortical thickness measure and the FA mean values in the left hippocampus for nine control subjects, but not for ADs (Figure 2).
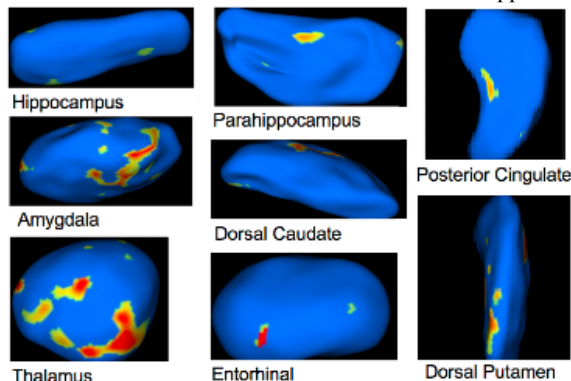

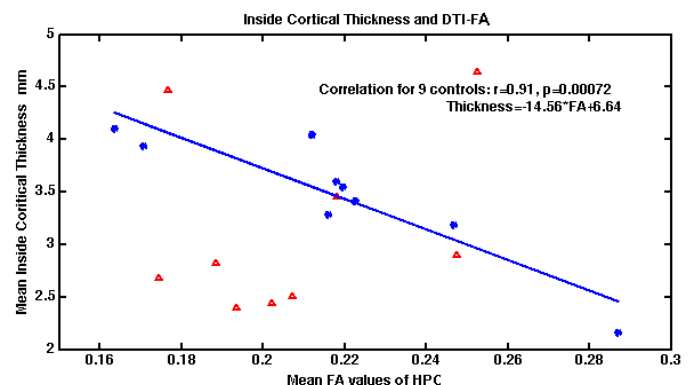**Fig.1** Shape difference between AD and control.

Fig.2 A significant negative correlation between thickness and FA measures in the hippocampus (HPC) in normal controls (blue), indicating a close relationship between the morphological and its underlying microstructual measurements. Such relationship is not seen in patients with AD (red).

Conclusion: The shape and thickness analysis is a promising tool for the improvement of the specificity of precise location of morphological changes of individual structures and for better clinical correlation; they may also elucidate morphological mechanism underlying different pathophysiological substrates. Our results demonstrated local morphological changes that involve several deep gray matter and MTL structures, consistent with the recent published article [2], suggesting that structural deformation analysis with the convergence of local shape, cortical thickness, and FA abnormalities may have potential to be a biomarker in early AD. Future morphological studies using shape and thickness analysis in different stages of AD are warranted.

References: [1] http://www.ia.unc.edu/dev. [2] Looi JCL, NeuroImage 2010; 51: 970-986.